



[Journal Homepage: -www.journalijar.com](http://www.journalijar.com)

INTERNATIONAL JOURNAL OF ADVANCED RESEARCH (IJAR)

Article DOI: 10.21474/IJAR01/22554
DOI URL: <http://dx.doi.org/10.21474/IJAR01/22554>



RESEARCH ARTICLE

LOCAL BEHAVIOR STUDY OF WATER AT THE OUTLET OF RECTANGULAR CHANNEL OF FLAT SOLAR COLLECTOR FOR THERMOSIPHON SOLAR WATER HEATER

C. W. Adihou^{1,2}, M. Aza-Gnandji³, M. Kple³, A. C. Houngan⁴ and M. Anjorin²

1. Process and Technological Innovation Laboratory (LaPIT) of the National Higher Institute of Industrial Technology, National University of Sciences, Technology, Engineering and Mathematics, Benin.
2. Laboratory of Applied Energetics and Mechanics (LEMA) University of Abomey-Calavi, Benin.
3. Rural Engineering Laboratory, National University of Agriculture, Benin.
4. Multidisciplinary Research Laboratory for Technical Education (LARPET), National University of Sciences, Technology, Engineering and Mathematics, Benin.

Manuscript Info

Manuscript History

Received: 04 November 2025
Final Accepted: 06 December 2025
Published: January 2026

Key words:-

Water channel, thermosiphon water heater, local temperature, local entropy, local velocity.

Abstract

This study deals with the water flow in a flat solar thermal collector with a rectangular channel for a thermosiphon water heater. It consists of determining the influence of the height of the water channel on parameters such as the water temperature at the outlet of the channel, the water outlet velocity of the channel and the generated entropy. To do this, the different equations of the local behavior of the water flow in the channel were estimated. These different equations were numerically solved by the finite element method through the Comsol Multiphysics software version 5.2a by considering three rectangular channels of width 1m and different heights (0.005 m, 0.01 m, 0.02 m). These different channels are exposed to two different fluxes namely 94 W/m² and 972 W/m² corresponding respectively to the lowest and highest solar flux of the study area. The results showed that the height of 0.01 m has an optimal speed and temperature. At this height, the generated entropy is lower than in the cases of heights of 0.005 m and 0.02 m.

"© 2026 by the Author(s). Published by IJAR under CC BY 4.0. Unrestricted use allowed with credit to the author."

Introduction:-

Natural convection heat exchange is an important phenomenon in technology and industry. In thermosiphon solar water heaters, heat exchange between the absorber and the heat transfer fluid occurs through natural convection. The advantages of systems with this heat transfer method are their simplicity, lower construction costs, good reliability, and quietness. Generally, the performance of solar water heaters is greatly influenced by the performance of the solar collectors. However, the performance of a solar thermal collector is reflected in the absorption of the maximum solar flux by the absorber, the reduction to a minimum of losses to the outside and the maximum exchange of heat between the absorber and the heat transfer fluid. Solar water heaters with flat absorbers are technologically simple to produce with locally available materials. But they have low efficiencies of around 40%. In order to increase the performance of solar collectors with flat absorbers, studies have been conducted by some researchers in recent years.

Corresponding Author:-C. W. Adihou

Address:-1. Process and Technological Innovation Laboratory (LaPIT) of the National Higher Institute of Industrial Technology, National University of Sciences, Technology, Engineering and Mathematics, Benin.2. Laboratory of Applied Energetics and Mechanics (LEMA) University of Abomey-Calavi, Benin.

Some studies on the geometric shape of the absorber or the hot water channel in the solar collector show their effects on the operation of solar water heaters. They reveal that the geometric shape of the absorber has a positive impact on the performance of the solar water heater [1, 2] because it influences the captured solar energy and the transmission of heat to the heat transfer fluid [3]. Serpentine-shaped water channels slightly improve the performance of solar water heaters compared to parallel tubes welded to a water collector. To increase the performance of solar water heaters by using parallel tubes welded to a collector, Mohammed Choukri Korti et al propose Zig-Zag tubes [5]. Other forms of water circulation channels in water heaters have been studied by other authors following experimental or numerical studies. Thus, Ho et al. [6], In 2007, conducted a theoretical study of the efficiency of a solar collector with rectangular fins placed inside circular water tubes that are positioned below the absorber. The tubes operate in pairs. Part of the water heated in one tube is reheated in the second tube. It is then mixed with cold water that enters the first tube. This system increased the outlet temperature of the heated water. Sekhar et al. [7] evaluated the heat loss coefficients in the flat-plate solar collector in 2009. The absorber of this collector is compact with cylindrical channels.

Diag [8] proposed in 2013 the compact flat absorber with rectangular and circular channels in order to increase the heat exchange performance between the absorber and the fluid. The results of his experimental tests show that the rectangular channel collector produces, compared to a conventional flat collector, an increase of 1.7 °C in temperature in a 300 liter water storage tank with 3.70 m² of collector surface. This result is confirmed by Anjorin et al who showed in a comparative study that a rectangular water channel has a significantly higher efficiency than water channels in a circular pipe [4]. Ramasamy et al. [9]. In 2015, Sivakumar et al. conducted an experimental study of the thermal performance of a solar collector with rectangular and circular fins placed inside circular water tubes. In this solar collector, the water tubes are placed above the absorber. For rectangular fins, the height and thickness are 5 mm and 2.5 mm, respectively. For circular fins, the diameter is 2.5 mm. The test results showed that the collector with an absorber equipped with fins has the effect of increasing the heat transfer, the thermal absorption coefficient, the thermal efficiency and the outlet temperature.

Also in 2015, Sivakumar et al. used the Computational Fluid Dynamics (CFD) method to simulate the transient heat transfer in a collector-storage type flat-plate solar water heater without fins and with fins of various shapes on the absorber completely immersed in water. [10]. These studies show improved heat transfer with an increase in the depth of the fins in the water. In 2017 Anjorin et al showed that rectangular water channels without fins have better performance compared to water channels with fins [1]. These different works focused on the global behavior of water heaters with a flat absorber. The present work focuses on the local behavior of solar collectors with a flat absorber whose water channel is rectangular. The objective is to analyze the local behavior of the operating parameters at the outlet of the channel. It is essentially a question of presenting the profiles of temperatures, speeds and entropies generated locally at the outlet of the collector as a function of the height of the water channel.

Materials and Methods:-

Mathematical models:-

The mathematical formulation of convection phenomena is based on equations linking the different parameters, namely: speed, pressure and temperature. These equations are obtained from the laws of conservation of mass, conservation of momentum and conservation of energy.

Law of conservation of mass:-

Also called the continuity equation, it is expressed by:

$$\frac{\partial \rho}{\partial t} + \frac{\partial}{\partial x_j} (\rho u_j) = 0 \quad (E.1)$$

Where $j=1, 2, 3$ (summation index)

Water is considered an incompressible fluid, equation (E.1) becomes:

$$\frac{\partial}{\partial x_j} (u_j) = 0 \quad (E.2)$$

Law Of Conservation Of Momentum:-

Also known as the Navier-Stokes equations, this law is written in the following form:

$$\frac{\partial}{\partial t}(\rho u_i) + \frac{\partial(\rho u_j u_i)}{\partial u_j} = F_i - \frac{\partial P}{\partial x_i} + \frac{\partial}{\partial x_j} \left[\mu \left(\frac{\partial u_i}{\partial x_j} + \frac{\partial u_j}{\partial x_i} \right) \right] \quad (E.3)$$

In this expression,

$\frac{\partial}{\partial t}(\rho u_i)$ represents the rate of change of the quantity of movement,

$\frac{\partial(\rho u_j u_i)}{\partial u_j}$ represents the net rate of transport of momentum by movement of the fluid along direction i,

F_i represents the volume forces along direction i,

$\frac{\partial P}{\partial x_i}$ represents the forces due to pressure,

$\frac{\partial}{\partial x_j} \left[\mu \left(\frac{\partial u_i}{\partial x_j} + \frac{\partial u_j}{\partial x_i} \right) \right]$ represents the net viscosity forces.

Law of conservation of energy:-

Called the energy equation, it is obtained by applying the first principle of thermodynamics for an incompressible Newtonian fluid.

$$\rho c_p \left[\frac{\partial T}{\partial t} + \frac{\partial}{\partial x_j} (u_j T) \right] = \frac{\partial}{\partial x_j} \left(\lambda \frac{\partial T}{\partial x_j} \right) + q + \mu \Phi \quad (E.4)$$

Or :

λ : Thermal conductivity,

c_p : Specific heat at constant pressure,

ρ : The density,

q : Heat generation per unit volume (volumetric heat density),

μ : Dynamic viscosity of the fluid,

F : Viscous dissipation.

Simplifying assumptions:-

The following assumptions were adopted:

Newtonian Fluid,

Continuous medium,

Two-dimensional flow (along x, y coordinates),

Laminar regime,

Viscous dissipation is negligible ($\mu \Phi = 0$),

Natural convection (buoyancy) is modeled using the Boussinesq approximation; it consists of considering that the variations in density are negligible at the level of all the terms of the momentum equations ($\rho = \rho_0$), except at the level of the gravity term. The variation of ρ as a function of temperature is given as follows[11]:

$$\rho = \rho_0 [1 - \beta (T - T_0)] \quad (E.5)$$

T_0 : Reference temperature

β : The coefficient of thermal expansion at constant pressure.

ρ_0 : Density of the fluid

The physical properties of the fluid (ρ , c_p , μ , k) are assumed to be constant.

Geometry of the problem considered:-

The system under study is the water channel of a solar collector for a thermosiphon water heater. This collector is inclined at 15° relative to the horizontal. The geometry of the water channel is shown in Figure 1.

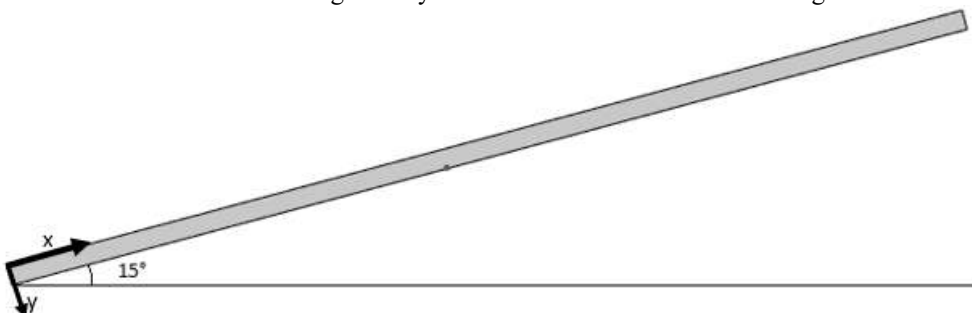


Figure 1: Physical representation of the field of study

It is water flowing between two parallel flat plates inclined at an angle Θ to the horizontal. The upper plate is heated by solar flux while the lower plate is thermally insulated. The water is deposited at the inlet of the plates without initial velocity at the beginning of the day. After a while in the sun, the initial velocity becomes non-zero due to the difference in water density created by the variation in water temperature. The water flows from the inlet to the outlet in an upward manner thanks to the temperature difference between the hot water particles and those of cold water. The length of the plates is 1 m.

Problem equations:-

After introducing the hypotheses given above, we can establish the different equations necessary for solving the problem considered in this study as follows:

Continuity equation:-

The continuity equation boils down to:

$$\frac{\partial u}{\partial x} + \frac{\partial v}{\partial y} = 0 \quad (E.6)$$

u and v are the components of the velocity field $V(u,v)$ in the x and y directions respectively.

Momentum equations:-

The momentum equations along the x and y axes are as follows:

$$\begin{aligned} \rho \left(u \frac{\partial u}{\partial x} + v \frac{\partial u}{\partial y} \right) &= - \frac{\partial p}{\partial x} - \rho g \cos(\theta) + \mu \left(\frac{\partial^2 u}{\partial x^2} + \frac{\partial^2 u}{\partial y^2} \right) \\ \rho \left(u \frac{\partial v}{\partial x} + v \frac{\partial v}{\partial y} \right) &= - \frac{\partial p}{\partial y} - \rho g \sin(\theta) + \mu \left(\frac{\partial^2 v}{\partial x^2} + \frac{\partial^2 v}{\partial y^2} \right) \end{aligned} \quad (E.7)$$

Pressure can be broken down into two parts: P_h for hydrostatic pressure and P_d for dynamic pressure caused by fluid motion. Dynamic pressure is unknown and determined by the equations for conservation of momentum and mass.

$$\frac{\partial p}{\partial x} = \frac{\partial p_h}{\partial x} + \frac{\partial p_d}{\partial x} \quad \text{et} \quad \frac{\partial p}{\partial y} = \frac{\partial p_h}{\partial y} + \frac{\partial p_d}{\partial y} \quad (E.8)$$

In our system, the hydrostatic pressure gradient is known and proportional to the gravitational field.

$$p_h = -\rho_0 g x \cos(\theta) - \rho_0 g y \sin(\theta) \quad (E.9)$$

By introducing equations (E.5), (E.8) and (E.9) into equations (E.7), we have:

$$\begin{aligned} u \frac{\partial u}{\partial x} + v \frac{\partial u}{\partial y} &= -\frac{1}{\rho} \frac{\partial p_d}{\partial x} + g \beta(T - T_0) \cos(\theta) + v \left(\frac{\partial^2 u}{\partial x^2} + \frac{\partial^2 u}{\partial y^2} \right) \\ u \frac{\partial v}{\partial x} + v \frac{\partial v}{\partial y} &= -\frac{1}{\rho} \frac{\partial p_d}{\partial y} + g \beta(T - T_0) \sin(\theta) + v \left(\frac{\partial^2 v}{\partial x^2} + \frac{\partial^2 v}{\partial y^2} \right) \end{aligned} \quad (E.10)$$

Energy equation:-

This equation is expressed by:

$$u \frac{\partial T}{\partial x} + v \frac{\partial T}{\partial y} = \alpha \left(\frac{\partial^2 T}{\partial x^2} + \frac{\partial^2 T}{\partial y^2} \right) \quad (E.11)$$

Boundary conditions:-

Solving the system of equations obtained previously requires the incorporation of boundary conditions for each dependent variable. The upper part is subjected to a heat flux, through the absorber, equal to q_{abs} and the adiabatic condition is imposed on the lower plate. Water enters the collector from the bottom at a temperature T_0 .

Its different conditions can be summarized in Table 1 below.

Table 1: Thermo-hydrodynamic conditions

Boundary	Hydrodynamic conditions	Thermal conditions
$y=0$ and $0 < x < L$	$U=V=0$	$\Phi = q_{abs} - h_p(T_{abs} - T_a)$ with $q_{abs} = \tau_v \cdot G \cdot h_p = 3 \text{ W.m}^2.\text{K}$
$y=h$ and $0 < x < L$	$U=V=0$	$\Phi = 0$
$x=0$ and $0 < y < h$	$U=V=0$	$T = T_0$
$x=L$ and $0 < y < h$	$\frac{\partial u}{\partial x} = \frac{\partial v}{\partial y} = 0$	$\frac{\partial T}{\partial x} = 0$

Calculation of the average Nusselt number:-

The convection heat transfer rate in an enclosure is obtained from the calculation of the Nusselt number. This is a dimensionless number important for the analysis of convection heat transfer. We are interested in the heat transfer at the heated part. The local Nusselt number is given by[12]–[13]:

$$Nu = \frac{ql}{\lambda_{eau}(T - T_0)} \quad (E.12)$$

The generated entropy:-

In a fluid flow under natural convection, the entropy generated is an energy degradation induced by thermal mechanisms involving temperature gradients. The mechanical contribution of the generated entropy is neglected. The local entropy generation per unit volume is expressed by[13]–[14]:

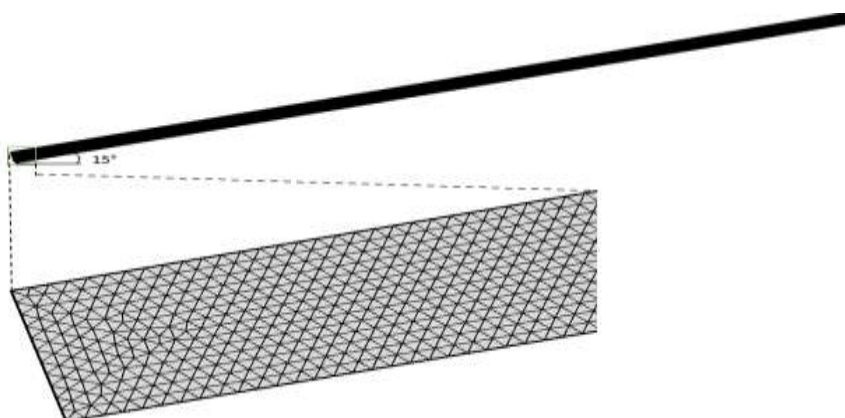
$$\dot{S} = \frac{\lambda_{eau}}{T^2} \left[\left(\frac{\partial T}{\partial x} \right)^2 + \left(\frac{\partial T}{\partial y} \right)^2 \right] \quad (E.13)$$

Numerical method:-

The resolution of the equations of a physical phenomenon of natural thermal convection is done by using a numerical method. The governing equations were solved numerically using the finite element method (FEM) implemented in COMSOL Multiphysics (version 5.2a). This method is the most widely used because it is very general and has a rigorous mathematical basis that is very useful, even on a practical level. Indeed, this mathematical basis makes it possible to predict up to a certain point the accuracy of the approximation and even to improve this accuracy, via adaptive methods. The finite element method is a special case of the Galerkin method for which the spaces V_h are easy to construct and for which the matrix A contains many zeros (we speak of a sparse matrix) which makes it possible to use efficient numerical methods for its inversion. The finite element method is above all an interpolation method. Thus, to approach a function, we divide its domain of definition into small elements and on each element, the local behavior of the function is represented by a simple function, such as a polynomial function for example.

The mesh:-

A mesh is a set of nodes and elements. A node is a geometric point supporting one or more unknowns. An element is a set of nodes associated with a geometrically simple domain. The mesh used in the Comsol environment is the triangular mesh as shown in Figure 2.

**Figure 1: Physical model mesh**

To minimize the error due to the mesh pitch, the smallest pitch available in the Comsol environment with the mention calibrate for fluid dynamics was chosen.

Results and Discussions:-

Our numerical simulations were carried out using Comsol Multiphysics version 5.2a software. This chapter presents all the simulation results concerning the study of the movement of water in its channel. It is useful to remember that this channel has a length "L" equal to 1 m and a height h which varies during the simulation. In this study, we presented the influence of the channel height on the temperature fields, isotherms, velocity fields and velocity contours.

Validation of results:-

Validation of the results is necessary because it allows us to give more credibility to the values found. This is done by comparing the results obtained by our simulations with other experimental or numerical results. The comparison was made with the results of the work of O.Miyatake and T. Fujii[15]. The latter expressed the local Nusselt number in natural convection between two infinite parallel plates ($h/L \rightarrow 0$) one of which is exposed to a constant flow q_1 and the other to a constant flow q_2 . The local Nusselt number at x is given by:

$$Nu(x) = \frac{\left(\frac{h}{x}\right) Ra_h^*}{\left[\left(\frac{h}{x}\right) Ra_h^*\right]^{\frac{1}{2}}} \times \frac{1 - \exp\left[-k\left(1 + \frac{q_2}{q_1}\right)^{\frac{3}{4}} \left(\frac{\left(\frac{h}{x}\right) Ra_h^*}{\left[\left(\frac{h}{x}\right) Ra_h^*\right]^{\frac{1}{2}}}\right)^{-\frac{2}{3}}\right]}{\left[24\left(1 + \frac{q_2}{q_1}\right)\right]^{\frac{1}{2}}} \quad (E4.15)$$

$$Ra_h^* = \frac{g\beta q h^4}{\lambda_f v \alpha} \quad (E4.16)$$

This correlation is valid for the Prandtl number $Pr = 10$. Not having work carried out under the same conditions of geometry and heat transfer fluid, we opted for this work which is carried out with geometric configurations closer to those of the present study. A comparison between the values of the local Nusselt number of the present study and those analytical obtained by the correlations of O. Miyatake and T. Fujii(equation E.15) for a height $h = 0.005$ m is made and the different values are grouped in table 2.

Table 2: Comparison of the Nusselt Numbers of the present study and those of the work of O. Miyatake and T. Fujii[15]

Imposed heat flux (W/m ²)	174	376	574	709	766
Present study	0.25	0.40	0.50	0.56	0.58
O. Miyatake and T. Fujii	0.37	0.49	0.61	0.68	0.69
Gap (%)	32.4	18.4	18.03	17.6	15.9

These differences between the values of the present study and those obtained by correlation of O. Miyatake and T. Fujii would reside in the nature of the heat transfer fluid. From these analyses, we can accept the results provided by code entered in the numerical simulation software used.

Results and interpretations:-

The results below show the speeds, temperatures and the local generated entropies for the heights h equal to 0.02 m, 0.01 m, 0.005 m and for the fluxes $G = 972 \text{ W m}^{-2}$ and $G = 94 \text{ W m}^{-2}$ corresponding respectively to the maximum solar radiation (radiation at 13 local hours or 12 hours GMT) and to the solar radiation at 8 local hours (07 hours GMT) for the month of September in Abomey-Calavi.

Local velocity:-

The local velocity profiles at the outlet of the water channel are shown in Figures 3 and 4.

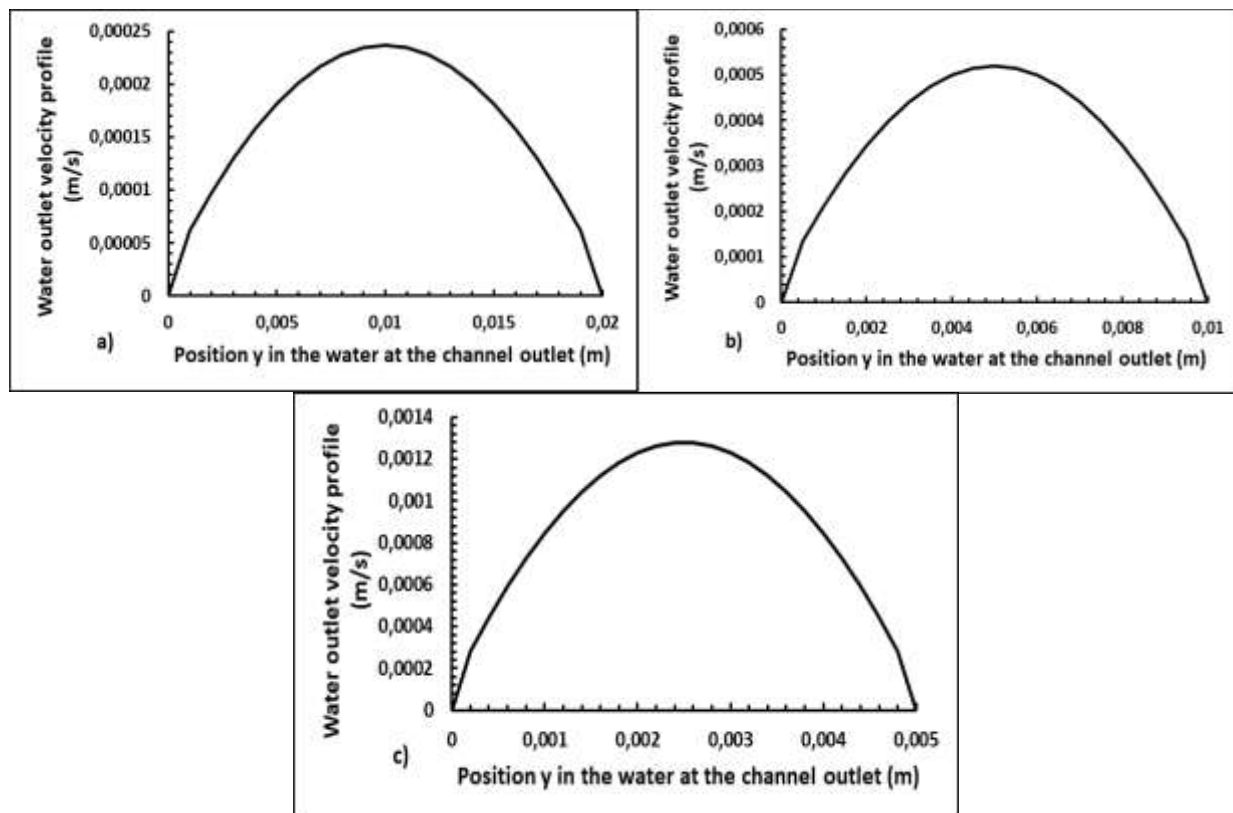


Figure 3: Water outlet velocity profile for a flux of 94 W/m^2 (8 hours local) with $h = 0.02 \text{ m}$ (a), $h = 0.01 \text{ m}$ (b) and $h = 0.005 \text{ m}$ (c).

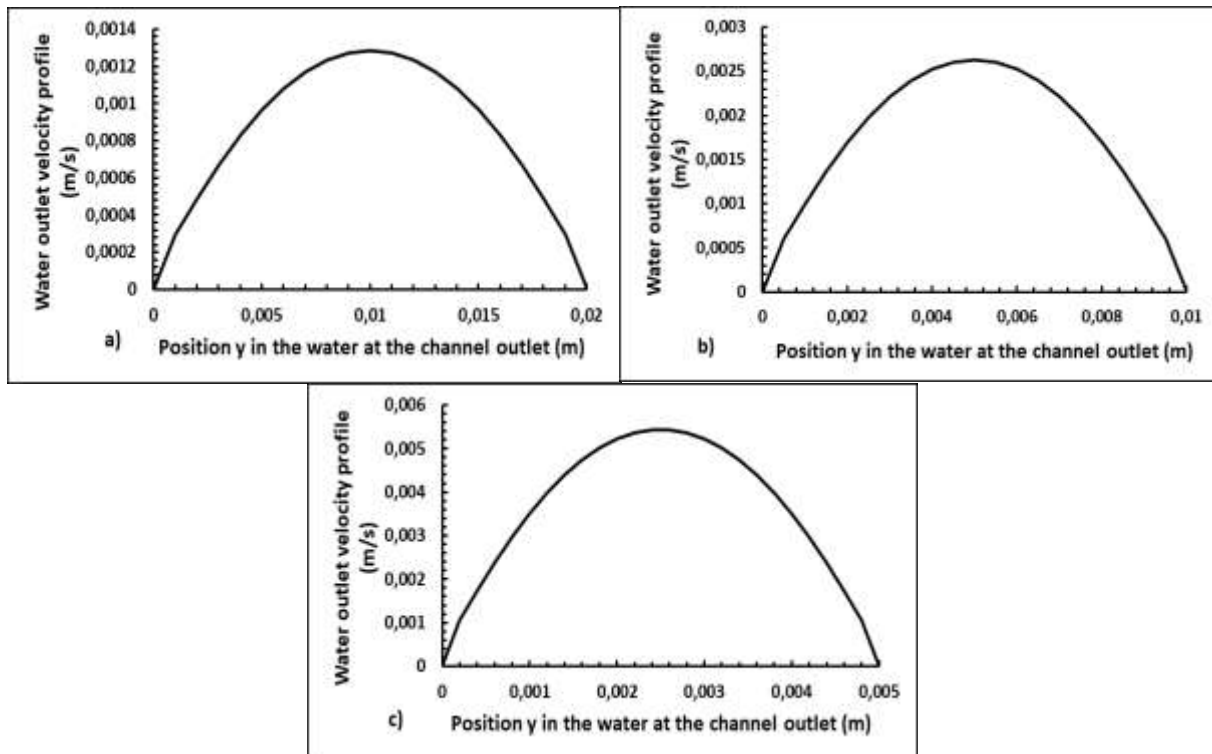


Figure 4: Water outlet velocity profile for a flux of 94 W/m^2 (8 hours local) with $h = 0.02 \text{ m}$ (a), $h = 0.01 \text{ m}$ (b) and $h = 0.005 \text{ m}$ (c).

These different graphs indicate zero velocities at the walls. The velocity increases as one moves away from the walls and reaches its maximum value in the middle of the channel. A progressively lower velocity towards the walls is the result to be expected because of the dynamic boundary layer phenomenon. This is due to the viscous force which becomes increasingly intense as one gets closer to the walls. This force is balanced by the inertial force and the gravitational force created by the difference in water temperature. The water velocity then exhibits a significant variation as a function of the channel height but a very small variation as a function of the channel length. This conclusion has been reached by many researchers who have worked in the field of flat plate convection. They even recommended neglecting the variation of the velocity in the longitudinal direction compared to its variation in the direction normal to the wall and expressed the fluid velocity as a function of the distance in the direction normal to the wall.

We can cite among others Michel Favre-Marinet and Sedat Tardu, Batchelor[16], [17]. We note that when the heat flow increases, the velocity increases with the exception of the velocities at the walls which are always zero. This increase in velocity is explained by a higher temperature difference created by the heat flow and also by the existence of a higher flow velocity at 1 p.m. than at 8 a.m. This will also create a higher gravitational force and will at the same time cause a higher viscous force at the walls. This phenomenon will increase the pressure drop in the circuit compared to the beginning of the day when the velocity is low. By changing the height of the channel to 0.01 m and 0.005 m, we also note that the velocity changes. On the other hand, we note a higher velocity gradient when the channel is thinner. For example, for a heat flux of 94 W/m², the 0.005 m channel shows a velocity gradient of 0.00075 m/s between 0 and 0.001 m, whereas in the 0.01 m and 0.02 m channels, the velocity gradients are 0.0005 m/s and 0.00035 m/s, respectively.

Local temperatures:-

Since the phenomena of temperature gradient and velocity are linked in natural convection, everything that is noticed at the level of velocity will be perceived in the behavior of the water temperature in the canal, a situation that Figures 5 and 6 highlight.

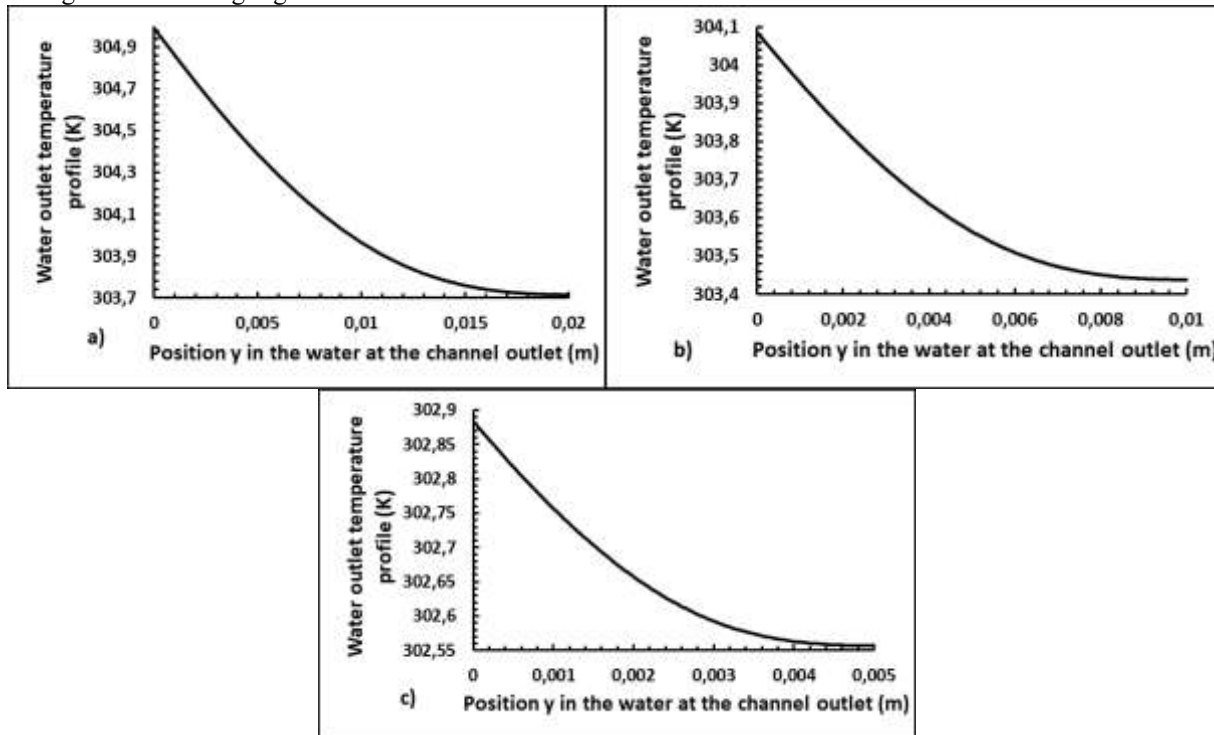


Figure 5: Water outlet temperature profile for a flux of 94 W/m² (8 hours local) with $h = 0.02 \text{ m}$ (a), $h = 0.01 \text{ m}$ (b) and $h = 0.005 \text{ m}$ (c).

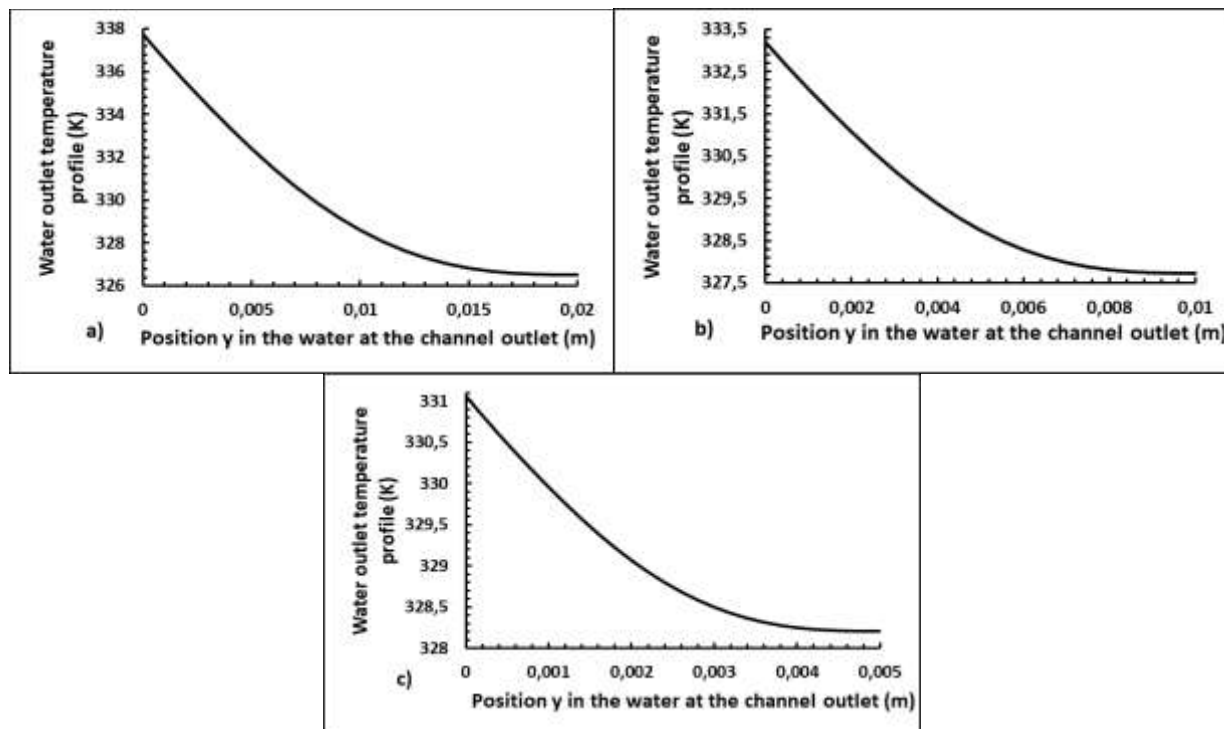


Figure 6: Water outlet temperature profile for a flux of 972 W/m^2 (8 hours local) with $h = 0.02 \text{ m}$ (a), $h = 0.01 \text{ m}$ (b) and $h = 0.005 \text{ m}$ (c).

Figures 5 and 6 reveal that the highest water temperatures are found near the hot wall and the lowest are found near the cold wall. This proves a phenomenon of more intense heat transfer near the hot wall and a weaker heat transfer far from the hot wall. This phenomenon also implies a higher entropy generated at the hot wall (Figures 7 and 8).

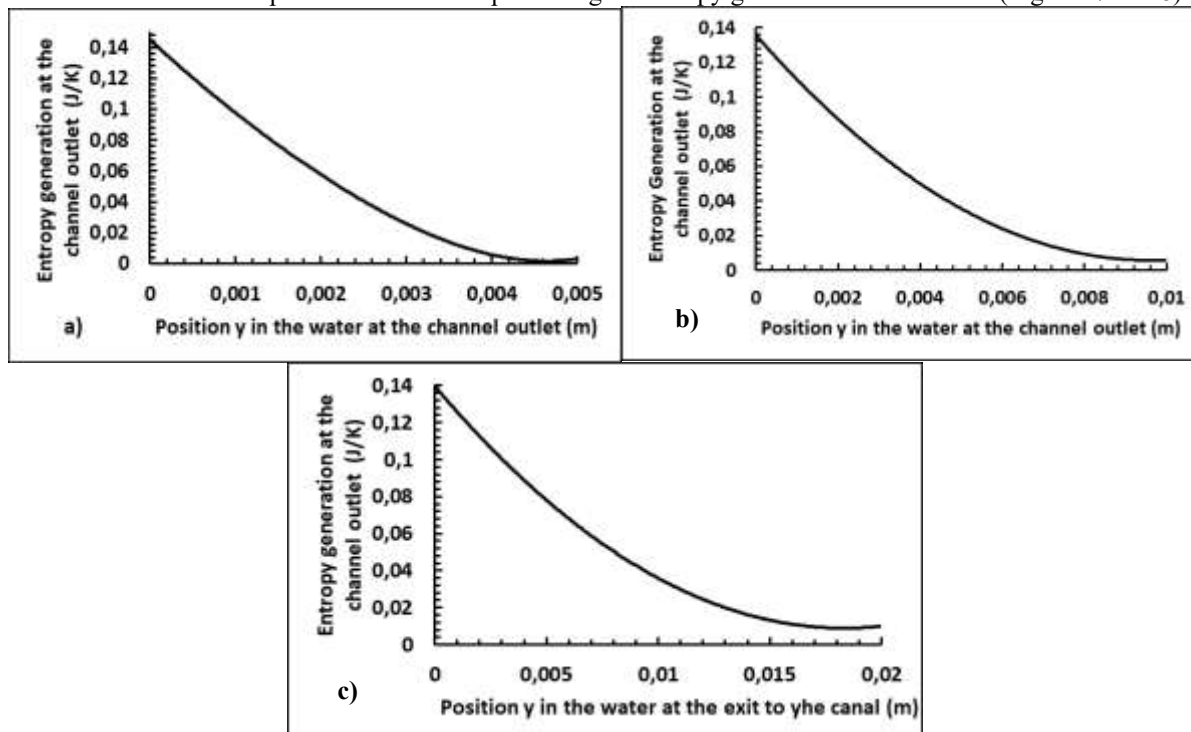


Figure 7: Entropy generated at the water outlet for a flux of 94 W/m^2 (8 hours local) with $h = 0.02 \text{ m}$ (a), $h = 0.01 \text{ m}$ (b) and $h = 0.005 \text{ m}$ (c).

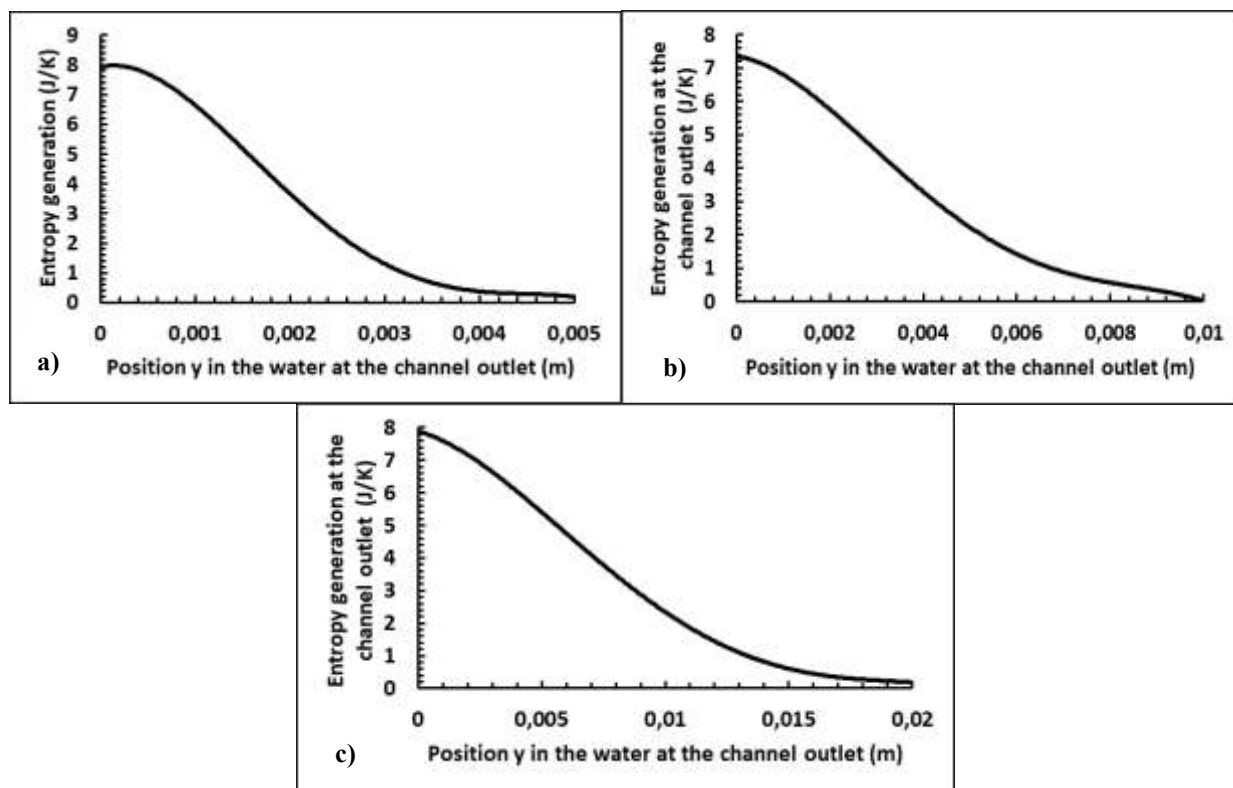


Figure 8: Entropy generated at the water outlet for a flux of 972 W/m^2 (8 hours local) with $h = 0.02 \text{ m}$ (a), $h = 0.01 \text{ m}$ (b) and $h = 0.005 \text{ m}$ (c).

The generated entropy is lower the further away from the hot wall. We also note that the generated entropy is high when the solar flux is high and it is low if the solar flux is low. In low solar radiation or high solar radiation, the generated entropy is lower in the case of the water channel with $h=0.01 \text{ m}$. Indeed, the entropies generated at the hot walls are 8.11 J/K , 7.33 J/K and 7.81 J/K respectively for $h=0.005 \text{ m}$, $h=0.01 \text{ m}$ and $h=0.02 \text{ m}$ for the flux of 972 W/m^2 . For the same flux (972 W/m^2) at the cold walls the entropies tend towards Zero. For a flux of 94 W/m^2 , the entropies generated for $h=0.005 \text{ m}$, $h=0.01 \text{ m}$ and $h=0.02 \text{ m}$ are respectively 0.15 J/k , 0.14 J/K and 0.14 J/K . At cold walls for the flux of 94 W/m^2 , the entropies tend towards Zero.

Through this study we can notice, with a high solar flux or a low solar flux, that:

- For the height $h=0.005 \text{ m}$, the water outlet temperature is low, the water flow rate is high and the generated entropy is high;
- For the height $h=0.02 \text{ m}$, the water outlet temperature is high, the water flow rate is low and the generated entropy is high;
- For the height $h=0.01 \text{ m}$, the water outlet temperature and the water flow rate present average values compared to those given with $h=0.005 \text{ m}$ and $h=0.02 \text{ m}$; but the generated entropy is lower.

It can be noted that for better performance of rectangular water channel water heaters, the recommended channel height is 0.01 m .

Conclusion:-

The local behavior of the water flowing through the solar collector was the subject of the study in this chapter. This local study is made on the analysis of the velocity, temperature and entropy profiles generated at the outlet of the channel by considering the operating parameters such as the height of the water channel and the heat flux. The various analyses made it possible to attest that the height of the channel greatly influences the performance of the collector. The present study then made it possible to realize the results related to the adoption of each height. For a better performance the height $h = 0.01 \text{ m}$ is recommended.

References:-

[1]: A. Malahimi., A. C. Wilfrid., H. C. Aristide., A. Christophe., D. Gerard. (2017). Optimization of the Fins Dimensions for the Absorber with Fins on a Compact Thermal Solar Collector by Entropy Generation Criterion. International Journal of Renewable Energy Research, 7(1), 58-67.

[2]: V. Badescu. (2006). Optimum fin geometry in flat plate solar collector systems. Energy Convers. Manag., 47(15–16), 2397–2413.

[3]: A. C. Wilfrid., A. Malahimi., H. C. Aristide., A. Christophe., S. A. Emile. (2020). Technological and Energy Optimization of the Height of Fins Placed on Flat Absorber for Solar Collector. Advanced Engineering Forum, 36, 1-12, doi:10.4028/www.scientific.net/AEF.36.1.

[4]: A. C. Wilfrid., D. A. Armand. V. E. Claude., A. Christophe., H. C. Aristide., A. Malahimi. (2022). Comparative study of the energy performance of two thermosiphon solar collectors with different waterchannels: channel in round tubes and channel under flat plate. Proc. of the International Conference on Electrical, Computer and Energy Technologies (ICECET), 9-10 December 2021, Cape Town-South Africa, 1-6.

[5]: M. C. KORTI., A. YOUSSEF., A. AKGUL., A. A. ALWAN., K. S. MOHSEN., J. ASAD., R. JARRAR., H. SHANAK., Y. MENNI., S. ABDULLAEV. (2023). Thermal Science, 27(48), 3143-3153.

[6]: C.-D. Ho., T.-C. Chen. (2007). Collector efficiency of double-pass sheet-and-tube solar water heaters with internal fins attached. 淡江理工學刊, 10(4), 323–334.

[7]: Y. R. Sekhar., K. V. Sharma., M. B. Rao. (2009). Evaluation of heat loss coefficients in solar flat plate collectors. ARPN J. Eng. Appl. Sci., 4(5), 15–19.

[8]: G. Diaz. (2013). Draft: Experimental characterization of an aluminum-based minichannel solar water heater. Proceeding of the ASME 2013 Summer Heat Transfer Conference, Minneapolis, USA, 14–19.

[9]: S. Ramasamy., P. Balashanmugam. (2015). Thermal performance analysis of the solar water heater with circular and rectangular absorber fins. Int J Innov Sci Technol Eng, 2(1) 596–603.

[10]: R. Sivakumar1., V. Sivaramakrishnan., M. Vivekenandan. (2015). CFD Study of an Integrated Collector – Storage Type Flat Plate Solar Water Heater Without and with Fins, Dimples and V-grooves in Absorber Surface. Int. J. Mech. Mechatron. Eng., 15(2), 30–35.

[11] : J. Padet. Principes des transferts convectifs, Seconde édition révisée.

[12] : S. Saha., G. Saha., M. Ali., M. Q. Islam. (2006). Combined free and forced convection inside a two-dimensional multiple ventilated rectangular enclosure. ARPN J. Eng. Appl. Sci., 1(3) 23–35.

[13]: M. Souad., (2015). Simulation numérique de la convection naturelle et la génération de l'entropie dans les cavités. Thèse, Université d'Oran.

[14] : A. Z. Sahin., R. Ben-Mansour., (2003). Entropy generation in laminar fluid flow through a circular pipe. Entropy, 5(5), 404–416.

[15]: O. G. Martynenko. (2005). Free-convective heat transfer: with many photographs of flows and heat exchange, 1. Ed. Berlin, New York: Springer,

[16]: G. K. Batchelor. (1954). Heat transfer by free convection across a closed cavity between vertical boundaries at different temperatures. Q. Appl. Math., 12(3), 209–233.

[17]: M. Favre-Marinet., S. Tardu. (2009). Convective heat transfer: solved problems. London: ISTE.